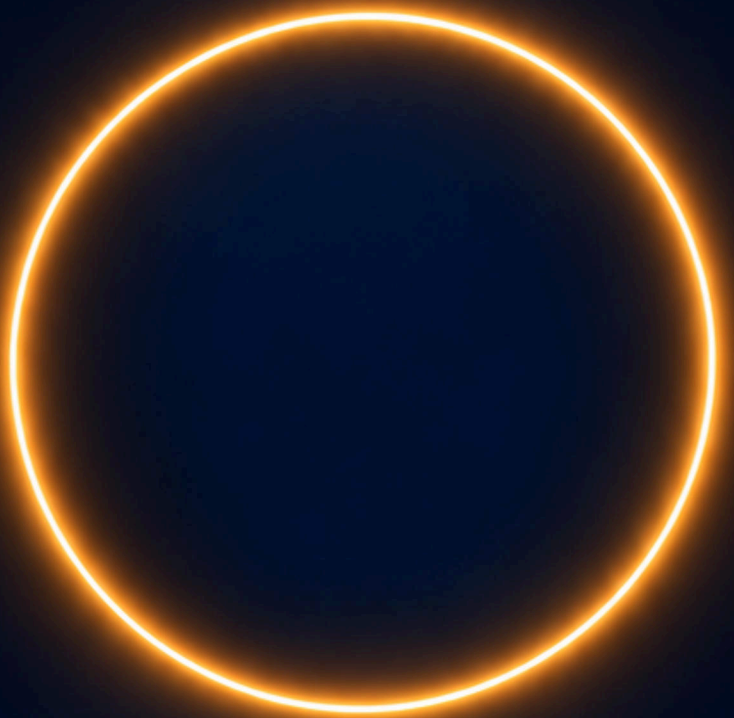
SCALE-TIME THEORY

THE GEOMETRY OF SCALE SPACE



André Dupke

Scale-Time Dynamics Research

André Dupke
Andalucía, October 30, 2026

scaletimedynamics.com - info@scaletimedynamics.com
Orcid | Academia | YouTube | Facebook

©2026 - Scale-Time Dynamics LLC - Licensed under CC BY 4.0
DOI: doi.org/10.5281/zenodo.23802558 - Version: 12.0

SCALE-TIME THEORY
The Geometry of Scale Space

ABSTRACT

Scale-Time Theory (STT) explores whether quantum ambiguity and classical stability can be understood as different sampling relations within one underlying scale space. The model represents scales by nested circular lanes. A shared phasor sweep places the same closed phase pattern on every lane, while its wavelength grows with radius. Comparing equal path lengths therefore gives the relative clock factor R_A/R_B.

Sampling the wrapped phase at intervals set by a reference lane produces the record $z_m = \exp[i(2\pi R_A m/R_B + \varphi)]$. This record admits an alias family of scales. A specified forward-branch reading reconstructs lanes larger than the sampler correctly; an amplitude-only record has the narrower reconstruction range $R_B > 2R_A$. Rational ratios produce repeating records, and finite records define coherence windows whose widths decrease with record length. Along an outward baseline, these windows define participation in a system relative to one reference and one observation window. Joining phase samples by straight segments introduces the interpolation error $1 - \cos(\pi R_A/R_B)$. At a chosen tolerance of about 7.6 percent, it settles at eightfold oversampling. The resulting transition band spans three octaves for phase records and two for amplitude records. These are conditional properties of the reading rule and tolerance.

Scale growth gives the exact kinematic law $R^2 = R_0^2 + (\alpha/\pi)S$. An optional displacement of a lane increases its path length and motivates a separate conjecture about mass. Connections with quantum behavior, acceleration, and entanglement remain research hypotheses. The paper provides a geometric and sampling model; physical carriers, interaction laws, and empirical calibration remain open.

Table of Contents

Abstract **2**

1. Purpose and scope **6**

1.1 The question 6

1.2 What is assumed and what is derived 6

2. Geometry and the shared sweep **8**

2.1 Lanes and positions 8

2.2 Baselines and the coordinate frame 8

2.3 Curved lanes and straight distance rays 9

2.4 Sweep and speed calibration 10

2.5 Closed imprint and scale modes 10

3. Clocks and equal-path comparison **12**

3.1 Local duration 12

3.2 Comparing equal paths 12

3.3 Curvature and lane deflection 13

4. What a sample retains **14**

4.1 The equal-path record 14

4.2 Why equal sweep increments give a different record 14

4.3 Synchronized phase and received phase 15

4.4 Phase and amplitude records 16

5. Aliasing and the readings of a record **17**

5.1 Hidden winding and the alias family 17

5.2 Correct reconstruction under a branch convention 17

5.3 Apparent forward, backward, and stationary order 18

5.4 Orientation and its ambiguity 18

5.5 Allowing both imprint senses 19

5.6 Additional information and exact recovery 19

6. Finite records and stroboscopic coherence **21**

6.1 One window function 21

6.2 Exact recurrence and finite-window locks 21

6.3 Sensitivity to the reference scale 22

6.4 Stroboscopic filtering 23

6.5 Participation in a system 23

7. Interpolation and the transition band **25**

7.1 Joining samples on the record circle 25

7.2 Amplitude dips and beats 26

7.3 A tolerance sets the settling threshold 26

7.4 Four relational regimes 27

8. Changing scale **28**

8.1 Scale acceleration and accumulated distance 28

8.2 Constant scale growth and the squared-scale law 28

8.3 An accelerating sampler 30

9. Displaced modes, mass, and energy **32**
9.1 An optional geometric extension 32
9.2 Clock corrections 32
9.3 The mass conjecture 33
9.4 Defined sweep energy 34
10. Physical interpretations & the research program **36**
10.1 The proposed quantum–classical connection 36
10.2 From recurrence to enduring systems 36
10.3 Acceleration, curvature, and spacetime 37
10.4 Shared modes and entanglement 37
10.5 What remains to be specified 39
10.6 A validation sequence 39
11. Conclusion **41**
Appendix A. Derivations **42**
A.1 Equal paths and local clock readings 42
A.2 The window and its bounds 42
A.3 Two samplers 43
A.4 Interpolation geometry 43
A.5 Growth and quadratic records 43
A.6 Displaced paths and clocks 44
A.7 The imaginary-time circle 46
Appendix B. Worked examples **47**
B.1 One sampler and ten lanes 47
B.2 An alias ladder and another sampler 47
B.3 Lock tolerance and participation 48
B.4 Scale growth 48
B.5 Interpolation and a slow beat 49
B.6 Displaced lanes 49
B.7 An octave ladder 49
Appendix C. Notation and assumptions **52**
C.1 Assumption index 52
C.2 Principal notation 53
Appendix D. Interpretive notes **55**
References **56**

And if you find the past in the large scales,
you will find the future in the small scales.

1. PURPOSE AND SCOPE

1.1 The question

STT asks whether the quantum–classical divide could be relational: whether the same underlying structure can appear ambiguous to one sampler and stable to another. Its starting elements are scale, orientation, and a shared phase order. The present model assigns lengths and durations to those elements and studies the records that result when one scale samples another. Companion work develops earlier forms of the framework [1, 2].

A filmed wheel gives the guiding example. Whole turns between frames are invisible. A wheel can appear still, move slowly forward, or turn backward, depending on its relation to the camera. Increasing the frame rate removes some ambiguities, while the appearance between frames still depends on how the images are joined. The record belongs to the wheel–camera pair.

In STT, the corresponding pair consists of two scale-lanes. The same number of phase cycles occupies each circumference, so a smaller lane carries more cycles per unit path. Equal-length paths on two lanes then contain different phase counts. Sampling one pattern at intervals set by the other produces the aliasing and stroboscopic relations developed below.

This construction is an explicit mathematical model. Its proposed interpretation beneath ordinary space and time remains hypothetical: Euclidean reference geometry is assumed, and an emergence of physical spacetime has yet to be supplied.

1.2 What is assumed and what is derived

The paper uses three status tags:

Tag	Meaning
[D]	A definition, postulate, convention, or result within the stated model
[C]	A proposed physical correspondence, accompanied by a test or development route
[I]	An interpretive picture or origin statement

The tag [D] marks status within the model; experimental support for an assumption is a separate matter. Postulates and conventions are named explicitly; their consequences are derived from them. Untagged exposition inherits the status of the statement it explains.

Sections 2–8 develop the circular-lane model. Section 9 adds an optional displaced lane and separates its geometry from the mass conjecture. Section 10 collects physical interpretations and the work needed to test them. Derivations, examples, notation, and interpretive notes appear in the appendices.

Four choices matter throughout: what a sample retains, which alias branch is read, how the record is interpolated, and which tolerance defines stability. These choices are stated where they enter. The model's eleven postulates and its additional conventions are indexed in Appendix C.

Radii have units of length, angles are in radians, and logarithms are natural. A dimensionless radius can instead be calibrated through $\ell = \chi R$; the equations below use $\chi = 1$. Lanes are denoted by A, B, G, systems by X, Y, and a reference radius by R_*. Write $d_{\mathbb{Z}}(x)$ for the distance from x to its nearest integer.

2. GEOMETRY AND THE SHARED SWEEP

2.1 Lanes and positions

[D] **Postulate 1: Scale space.** A scale slice has radius $R > 0$. Its circular representation carries a scale-lane of circumference

$$C(R) = 2\pi R$$

The reference plane is Euclidean. Radial displacement changes scale; angular displacement changes orientation. A selected position is

$$P(R,\beta) = (R\cos\beta, R\sin\beta) \qquad \beta \in [0,2\pi)$$

or $Re^{i\beta}$ in complex notation. The local scale-space chart is $(0,\infty) \times S^1$.

The circular representation supplies size, one internal angular coordinate, and a lane. The intended finite, borderless, two-dimensional slice requires a further internal direction at fixed scale. That completion is open; the radial coordinate changes scale and therefore leaves the second internal direction to be specified.

2.2 Baselines and the coordinate frame

[D] **Postulate 2: Baselines and systems.** The sweep opens outward channels from the center. A baseline is a channel at a retained orientation β_X, along which the common signal reaches smaller scales before larger ones. The sweep renews it once per turn. A system consists of the slices whose records are coherent with a reference slice over a selected record length, according to Section 6.5.

A system is written

$$\mathcal{S}_X = (\mathcal{R}_X, \beta_X)$$

where membership in $\mathcal{R}_X$ depends on the reference and the record length. In the system's own frame, $\beta_{\text{loc}} = \beta - \beta_X$, its baseline is the positive x-ray and its positions are $(R,0)$. For two systems, or lanes carried by them, relative orientation is $\Delta\beta_{B|A} = \beta_B - \beta_A$.

[D] **Postulate 3: Principal rays.**
The four rays x^+, y^+, x^-, y^- represent angles $0, \pi/2, \pi, 3\pi/2$. Multiplication by i advances through them in the forward order. Only x^+ has the physical role assigned to the baseline. The remaining rays complete the coordinate notation.

A baseline retains its orientation while the sweep turns. Within the model, relative orientations carry the content: a common rotation of every β_X, together with the same shift of the sweep's phase origin, leaves imprint phases, records, and distances unchanged. Each β_X is therefore measured from the sweep's direction at $\Theta = 0$, while orientations relative to other systems are intrinsic. The mechanism that holds a baseline at its orientation, and the transmission law along it, remain open (Section 10.2). The synchronized phase reference introduced below must also be distinguished from a signal received after a delay; Section 4.3 makes that distinction explicit.

2.3 Curved lanes and straight distance rays

[D] **Postulate 4: Distance rays.** Systems follow their lanes relative to the sweep. Observation, interaction, and displacement are assigned to straight segments between positions, called distance rays.

The distance between two positions is

$$d^2_{B|A} = R_A^2 + R_B^2 - 2R_A R_B \cos \Delta\beta_{B|A}$$

It is symmetric and unchanged by rotating the reference frame. On one baseline it is $|R_B - R_A|$; at a quarter turn it is $\sqrt{R_A^2 + R_B^2}$; at opposite orientations it is $R_A + R_B$.

At equal radii, the straight distance is the chord $2R|\sin(\Delta\beta/2)|$. The shorter lane arc has length $R|\Delta\beta|$ when $\Delta\beta \in (-\pi, \pi]$. In particular,

$$D(R) = 2R \qquad \frac{C(R)}{D(R)} = \pi \qquad \kappa_R = \frac{1}{R}$$

Here π is the global circumference-to-diameter ratio; κ_R is local lane curvature. They describe different geometric properties. Over a path s, the lane turns through s/R.

2.4 Sweep and speed calibration

[D] **Postulate 5: Phasor sweep.** All lanes share the ordering phase

$$\mathscr{P}(\Theta) = e^{i\Theta} \qquad \Theta = \Omega t \qquad T_{\mathscr{P}} = \frac{2\pi}{\Omega}$$

The parameter t is sweep time. Its identification with a laboratory clock is a separate physical question.

[D] **Postulate 6: Speed calibration.** Choose a reference lane R_*. Its circumference per sweep period defines

$$c = R_*\Omega$$

This fixes the relation between the model's length and time units. Identifying c with the measured speed of light requires the calibration discussed in Section 10.

2.5 Closed imprint and scale modes

[D] **Postulate 7: Imprint.** Every lane carries the synchronized phase pattern

$$M(t, R, \beta) = A_0 \sin\Phi \qquad \Phi = N(\Theta - \beta) + \phi_0$$

The complex representation is $A_0 e^{i\Phi} = A_0 \mathscr{P}^N e^{-iN\beta} e^{i\phi_0}$. Its sine and cosine are coordinates of one phase. After normalization, $e^{i\Phi}$ lies on the imprint-phase circle. This is a representation of phase, distinct from the geometric lane on which the imprint is defined.

The imprint must close after one circuit:

$$e^{-iN(\beta+2\pi)} = e^{-iN\beta} \qquad N \in \mathbb{Z}$$

Integer winding follows from this closure requirement. The main model uses one common $N \geq 1$ and one sense of advance. The imprint on a lane is its scale mode. Each mode has

$$\lambda_R = \frac{2\pi R}{N} \qquad \nu_R = \frac{N}{2\pi R}$$

The phase-order density ν_R counts cycles per unit path; the phase in radians advances at $2\pi\nu_R$. Small lanes carry denser patterns, while larger lanes carry stretched copies of the same angular pattern.

A position on a fixed baseline stays at β_A. In the frame rotating with the sweep its coordinate is $\psi_A = \beta_A - \Theta$, so it traverses the lane once per sweep turn relative to the pattern. The clock at that position reads $N(\Theta - \beta_A) + \phi_0$. A point rotating with the pattern would read a constant phase.

[I] The sweep can be pictured as a central source with intensity $I_0[1 + \sin(N\Theta + \phi_0)]$. Its pulse sequence is distributed around each lane and outward along baselines. This picture motivates the imprint and leaves the physical source and its transport mechanism to be specified.

3. CLOCKS AND EQUAL-PATH COMPARISON

3.1 Local duration

[D] **Postulate 8: Local duration.** A sweep increment covers lane path $ds = R\,d\Theta$. Its local duration is

$$d\tau_R = \frac{ds}{c} = \frac{R}{c}\,d\Theta = \frac{R}{R_*}\,dt$$

Thus $\tau_{R_*} = t$ up to a choice of origin. A turn on lane R lasts $T_R = 2\pi R/c$ in local duration. Since it contains N imprint cycles, the local clock frequency is

$$f_R = \frac{Nc}{2\pi R} \qquad f_R \lambda_R = c$$

All lanes advance by N cycles per sweep turn. Their local frequencies differ because their paths, and therefore their assigned local durations, differ.

3.2 Comparing equal paths

[D] **Postulate 9: Comparison.** Compare lanes over equal path lengths beginning at their baselines, or equivalently over equal elapsed local durations. Count both from a common sweep event.

The relative clock factor of lane B with respect to lane A is

$$r_{B|A} = \frac{\nu_B}{\nu_A} = \frac{f_B}{f_A} = \frac{R_A}{R_B} = \frac{\kappa_B}{\kappa_A}$$

For example, a path equal to one circuit of A covers half a circuit of a lane with radius $2R_A$. It contains half as many imprint cycles. A comparison by full circuits would return N cycles on every lane and carry the shared order alone.

Equal local durations generally correspond to different sweep phases: after local duration τ, the phases are $c\tau/R_A$ and $c\tau/R_B$. By contrast, over one common sweep increment,

$$\frac{\Delta s_B}{\Delta s_A} = \frac{R_B}{R_A} \qquad r_{B|A}\frac{\Delta s_B}{\Delta s_A} = 1$$

Shared sweep order and equal-path measure are therefore distinct comparisons. The clock factors obey

$$r_{A|A} = 1 \qquad r_{A|B} = \frac{1}{r_{B|A}} \qquad r_{G|A} = r_{G|B} r_{B|A}$$

In the logarithmic scale coordinate $u = \ln(R/R_*)\$, \$r_{B|A} = e^{u_A - u_B}$ and composition becomes addition of logarithmic ratios. Equal octaves occupy equal intervals in u. The letter u keeps this meaning in this section and in Appendix B.7, which follows an exactly commensurate octave ladder; Appendix A.4 uses it for an interval fraction.

3.3 Curvature and lane deflection

[D] The clock relations can be written entirely in terms of lane curvature:

$$\nu_R = \frac{N\kappa_R}{2\pi} \qquad f_R = \frac{Nc\kappa_R}{2\pi}$$

Starting from $(R,0)$, a path s reaches $(R\cos(s/R), R\sin(s/R))$. Its coordinate along the baseline falls toward the origin by

$$h(s) = R\left(1 - \cos\frac{s}{R}\right) = \frac{s^2}{2R} - \frac{s^4}{24R^3} + \cdots$$

With $s = c\tau$, the leading departure is $h \simeq a_R\tau^2/2$, where

$$a_R = \frac{c^2}{R} \qquad f_R = \frac{Na_R}{2\pi c}$$

The quantity a_R is the lane deflection: curvature expressed through the assigned local speed. It concerns a lane of fixed radius. Scale acceleration, introduced in Section 8, changes the radius itself.

4. WHAT A SAMPLE RETAINS

4.1 The equal-path record

[D] **Postulate 10: Sampling.** A slice samples the phase pattern of another slice over equal paths. Its own wavelength sets the interval. For fixed sampler A, sample m reads the phase of lane B at path $m\lambda_A$ from its baseline, against the direction of imprint travel, at the common sweep event. The retained quantity is phase modulo 2π.

This is a whole-lane comparison, made with one retained phase per sample and the baseline as its only physical ray. Access to wrapped phase is an explicit assumption of this postulate, beyond the definition of a clock.

Because the pattern travels at c in local measure, the phase found a path s behind the baseline reaches that position after local duration s/c. Spatial sampling at one sweep event therefore gives the same sequence as reading B at elapsed local durations

$$\tau_B = m\Delta\tau_A \qquad \Delta\tau_A = \frac{\lambda_A}{c} = \frac{1}{f_A}$$

The resulting relational record is

$$z_m = \exp[i(2\pi r m + \varphi)] \qquad r = \frac{R_A}{R_B} \quad m = 0,1,2,\ldots$$

The constant φ collects the initial phase, relative orientation, and fixed transmission delays. Each interval spans r cycles of B. Complete cycles between samples are hidden.

One circuit of A supplies N sampling intervals and covers the fraction R_A/R_B of B's circumference. With $N = 12$, lanes at R_A,$2R_A$,$3R_A$,$4R_A$ contribute respectively 12,6,4,3 cycles over that path. Count a record on a half-open path to obtain N samples per circuit; including the final endpoint gives $N + 1$.

4.2 Why equal sweep increments give a different record

One sampling interval of A corresponds to sweep increment $2\pi/N$. Over that same sweep increment every lane advances by one imprint cycle. A record taken synchronously in sweep time is therefore stationary for every radius.

The nontrivial ratio r enters through the equal-path rule. Its temporal equivalent compares equal local durations on the two lanes, which generally occur at different sweep phases. The record above is thus a defined relational comparison, distinct from an ordinary simultaneous time series in the global parameter t. A physical implementation of this comparison remains to be specified.

Self-sampling gives $r = 1$ and a stationary record. Reciprocal sampling gives $r_{A|B} = 1/r_{B|A}$, so two unequal lanes can produce different kinds of record when their roles are exchanged.

4.3 Synchronized phase and received phase

The imprint of Section 2.5 is a synchronized reference: at one sweep event every radius on a ray carries the same reference phase. If transmission to radius R takes sweep time $T(R)$, the received phase is instead

$$\Phi_R^{\mathrm{rec}}(t, \beta) = N[\Omega(t - T(R)) - \beta] + \phi_0$$

On a common ray,

$$\Phi_B^{\mathrm{rec}} - \Phi_A^{\mathrm{rec}} = -N\Omega[T(R_B) - T(R_A)]$$

For fixed radii and fixed delays this is a constant offset. It preserves the phase increments, coherence magnitudes, and interpolation error derived below. For example, $T(R) = R/c$ in sweep time gives offset $-NR/R_*$.

A calibrated offset can nevertheless add scale information. With $N = R_* = R_A = 1$, lanes at $R_B = 4$ and 0.8 have identical sampled phase increments but delay offsets -4 and -0.8 radians. A known source phase distinguishes their complete records. Accordingly, alias families below are families of phase increments; identical complete records also require the constant phase to be unknown, adjustable, or removed.

A changing transmission path can change the phase increment itself. The acceleration formulas in Section 8 describe the defined reference record; variable propagation delays require an additional model.

4.4 Phase and amplitude records

A phase record retains the angle Φ modulo 2π. Writing it as $\cos\Phi + i\sin\Phi$ supplies two coordinates for that one circular variable. If the sampler retains only the instantaneous imprint value, normalized by A_0, it instead produces

$$x_m = \sin(2\pi r m + \varphi)$$

For integer m,

$$\sin(2\pi r m + \varphi) = \sin[2\pi(1 - r)m + \pi - \varphi]$$

With a free initial phase, a real-valued record therefore identifies a rotation with its mirror. It can show repetition and stationarity, while signed circular motion requires the phase record or information beyond the sequence. A separately known source phase can supply additional information.

5. ALIASING AND THE READINGS OF A RECORD

5.1 Hidden winding and the alias family

[D] Write

$$r = w + \rho \qquad w = \lfloor r \rfloor \qquad 0 \le \rho < 1$$

The integer w is hidden winding and ρ is the residual. Since $e^{2\pi i w m} = 1$, the record's phase increments depend on r only through ρ. This is ordinary sampling aliasing expressed as a scale relation [3, 4].

For sampler A, all compatible positive radii form

$$\mathscr{A}_{B|A} = \left\{ \frac{R_A}{\rho + j} : j = 0,1,2,\ldots \right\}$$

with $j \ge 1$ when $\rho = 0$. The true lane occupies rung $j = w$. For $\rho = 0$, the family is the harmonic ladder $R_A, R_A/2, R_A/3, \ldots$, whose records are all stationary.

5.2 Correct reconstruction under a branch convention

[D] **Forward-branch convention.** Read the record on the branch $0 < r < 1$, consistent with the assumed forward imprint sense. For $\rho > 0$, assign

$$R^{\mathrm{app}}_{B|A} = \frac{R_A}{\rho}$$

This is the largest member of the alias family. For a stationary record, adopt $R^{\mathrm{app}} = \infty$ as a zero-frequency convention. Infinity is a limiting reading beyond the positive-radius harmonic ladder.

The convention returns the true radius exactly when $R_B > R_A$. At or below R_A, the true radius occupies a hidden rung. In this sense a sampler resolves every flatter lane and aliases every lane at least as curved as itself.

Correct branch reconstruction and identification from data are different. For $R_A = 1$, radii 4 and 0.8 give ratios 0.25 and 1.25. From equal initial phases they produce identical records of every length, and the forward reading returns 4 for both. A known admissible-

scale range, a calibrated phase offset, or another sampler is needed to identify the actual member.

An amplitude-only record with free initial phase adds the mirror branch

$$\left\{ \frac{R_A}{1-\rho+j} : j = 0,1,2,\ldots \right\}$$

The two branches coincide at $\rho = 0$ and $\rho = 1/2$. The conventional amplitude reconstruction range is $R_B > 2R_A$, corresponding to less than half a cycle per sample. This is the familiar Nyquist boundary in the present variables.

5.3 Apparent forward, backward, and stationary order

[D] **Minimal-step reading.** Choose the nearest integer winding,

$$\delta = r - \left\lfloor r + \frac{1}{2} \right\rfloor \qquad -\frac{1}{2} \le \delta < \frac{1}{2}$$

The apparent phase step is $2\pi\delta$. At half-integer ratios the floor convention gives $\delta = -1/2$, the case of undecided sense. A numerical implementation should declare a tolerance and mark every ratio whose $|\delta|$ lies within that tolerance of $1/2$ as undecided, so that the sign at the boundary follows the declared rule rather than floating-point rounding.

Residual step	Apparent order
$\delta = 0$	stationary
$0 < \delta < 1/2$	forward
$-1/2 < \delta < 0$	backward
$\delta = -1/2$	alternating opposite phases; sense undecided

For $R_A < R_B < 2R_A$, the forward-branch reading returns the true scale while the minimal-step reading runs backward. The lane advances by more than half a cycle per sample; the minimal-step reading takes the shorter path in the opposite direction. The underlying sweep still advances forward.

5.4 Orientation and its ambiguity

At equal sweep phase, the synchronized imprint offset between baselines is $-N\Delta\beta$. Phase alone resolves orientation only modulo $2\pi/N$.

N modulo 4	Distinguishable principal rays
1 or 3	all four
2	x^+, x^- and y^+, y^-
0	one phase class

Residues 1 and 3 assign opposite quarter-turn offsets. This ambiguity concerns imprint readings. The underlying rays remain geometrically distinct, and the distance formula uses their full angular separation. Received phase comparisons additionally require the delays in Section 4.3 to be accounted for.

5.5 Allowing both imprint senses

[C] The main model assumes one sense. An extension could permit $\tilde{r} = \pm r$, with record $e^{i(2\pi\tilde{r}m+\varphi)}$. At $r = 1/2$, the two senses give exactly the same record from the same initial phase, independent of record length or noise.

Within the known band $-1/2 < \tilde{r} < 1/2$, phase sampling determines both magnitude and sense, giving the reconstruction boundary $R_B > 2R_A$. Outside that band, integer aliases remain: $\tilde{r} = 0.75$ and -0.25 are indistinguishable. This extension requires a physical definition of the two senses before sampling; two physical modes need evidence beyond apparent reversal. Its test would compare signed modes under a stated admissible band and a specified readout model.

5.6 Additional information and exact recovery

[D] Two consecutive noiseless phase samples determine the residual exactly:

$$z_{m+1}\overline{z_m} = e^{2\pi i r}$$

For amplitude samples,

$$x_{m+1} + x_{m-1} = 2\cos(2\pi r)x_m$$

A triple with nonzero middle value determines $\cos(2\pi r)$, leaving the mirror ambiguity. A triple whose middle value vanishes leaves that relation open, and any triple $(x_{m'-1}, x_{m'}, x_{m'+1})$ with $x_{m'} \neq 0$ supplies it. Two consecutive samples vanish together only

when $2r$ is an integer and the alignment places every sample on a zero crossing, so that the entire amplitude record vanishes, as at a Nyquist zero-crossing alignment.

A second sampler resolves the integer ambiguity in the exact noiseless model. Let $\mu = R_{A'}/R_A$. If μ is irrational, the two alias families share exactly one radius. If $\mu = p'/p$ in lowest terms, they determine r modulo p. Appendix A.3 gives the proof. Finite precision and noise can leave near-coincident candidates unresolved, as Appendix B.2 illustrates.

If admissible radii satisfy $R \geq R_{\min}$, the number of candidates is finite. For a record with at least one admissible member,

$$K = \left\lfloor \frac{R_A}{R_{\min}} - \rho \right\rfloor + 1 \quad (\rho > 0) \qquad K = \left\lfloor \frac{R_A}{R_{\min}} \right\rfloor \quad (\rho = 0)$$

The sampling construction itself leaves the weighting of these alternatives open.

6. FINITE RECORDS AND STROBOSCOPIC COHERENCE

6.1 One window function

[D] A record of length L contains samples $m = 0,\ldots, L-1$. Its basic window function is

$$\Gamma_L(x) = \left| \frac{1}{L} \sum_{m=0}^{L-1} e^{2\pi i x m} \right| = \frac{|\sin(\pi L x)|}{L\,|\sin(\pi x)|}$$

with $\Gamma_L(x) = 1$ at integer x. It governs three quantities:

Quantity	Expression	Meaning
Record overlap	$O_L(r, r') = \Gamma_L(r - r')$	agreement after disregarding a constant phase offset
Order-q coherence	$\Gamma_L^{(q)}(r) = \Gamma_L(qr)$	how closely $z_m q$ holds one phase
Magnitude of the mean record	$\lvert\langle z\rangle_L\rvert = \Gamma_L(r)$	the stationary component of the record

For $y = d_{\mathbb{Z}}(x) > 0$,

$$\Gamma_L(x) \le \frac{1}{2Ly} \qquad y \le \frac{1}{2L} \implies \Gamma_L(x) \ge \frac{2}{\pi}$$

Appendix A.2 derives these bounds. Records whose residual separation is at least $1/L$ have overlap at most $1/2$. The overlap width is therefore of order $1/L$, often written $\Delta\rho\, L \sim 1$.

This width describes a comparison of records, distinct from an uncertainty in the residual: two exact phase samples already determine that residual. An estimation precision follows only after specifying noise, quantization, or a decision criterion.

6.2 Exact recurrence and finite-window locks

An integer ratio produces a stationary image. A reduced rational ratio $r = p/q$ produces a periodic image of q equally spaced phases, visited in the order set by p. An irrational ratio produces phases that become equidistributed on the circle as the record grows [5].

For $L \ge 2$, order-q coherence is exactly one when qr is an integer. A finite record is defined to be locked at order q when

$$d_{\mathbb{Z}}(qr) \le \frac{1}{2L}$$

Near a reduced ratio p/q, this gives the window

$$\left| r - \frac{p}{q} \right| \le \frac{1}{2qL}$$

Its coherence is at least $2/\pi$. Integer locks have the widest windows, followed by orders two and three. These are kinematic recurrence windows; a dynamical attraction toward a lock would require coupling (Section 10.2).

Define the lowest locking order at length L by

$$q_L(r) = \min \left\{ q \ge 1 : d_{\mathbb{Z}}(qr) \le \frac{1}{2L} \right\}$$

Dirichlet approximation gives $q_L \le 2L - 1$, so every finite record locks at some order [6]. What distinguishes useful recurrence is an order small compared with the record length. The classification below adopts $q_L^2 \le L$ as its low-order cutoff.

For rational $r = p/q$, $q_L = q$ once $L > q/2$. For irrational r, q_L grows without bound, through increasingly accurate rational approximations; continued fractions describe this growth [7]. The golden ratio supplies the familiar Fibonacci example.

A finite-window lock allows residual drift. At $r = 2.003$ and $L = 100$, the record is locked at order one with coherence about 0.858, although its phase drifts through 0.297 cycles between its first and last samples.

6.3 Sensitivity to the reference scale

A relative change $\varepsilon = \Delta R_A / R_A$ changes the ratio by $\Delta r = r\varepsilon$. Starting from an exact order-q lock, it stays inside that window when

$$|\varepsilon| \le \frac{1}{2qLr} = \frac{R_B}{2qLR_A}$$

At fixed order and record length, a lock to much finer structure requires tighter control of the sampler. Increasing record length also narrows the tolerance. Coherence is always a statement about a specified window and perturbation scale.

6.4 Stroboscopic filtering

The mean record retains two contributions at substantial magnitude. Integer ratios give $|\langle z\rangle_L| = 1$, preserving the harmonic ladder. Very small ratios satisfy

$$0 < r \le \frac{1}{2L} \quad \Longleftrightarrow \quad R_B \ge 2L R_A$$

and give $|\langle z\rangle_L| \ge 2/\pi$. These coarse lanes change little during the window. Other ratios obey the upper bound $1/[2L\, d_{\mathbb{Z}}(r)]$.

The stationary part of a record can therefore come from a fast pattern aliased onto an integer lock or from a sufficiently slow pattern. Distinguishing those origins requires information beyond the arithmetic.

6.5 Participation in a system

[D] **Participation rule.** Fix a reference slice A, its baseline, and record length L. A slice B participates in its system when

$$q_L(R_A/R_B)^2 \le L$$

The reference participates through self-sampling. Membership is assessed directly against that reference, independent of approximate locking between other pairs.

This rule defines a finite-window collection. For $R_B = 20R_A$, $q_L = 20$ at both $L = 100$ and 400, so the slice is excluded at the first length and included at the second. An enduring system requires a persistence or coupling rule beyond this classification.

Order-q coherence also differs from equality of phase at every sample. At $r = 1/3$, the mean of z_m vanishes over complete three-sample periods, while the magnitude of the mean of z_m^3 is one. The rule measures recurrence.

Along the baseline, positive rational lock centers lie at

$$R_B = \frac{q}{p} R_A$$

with widths specified in the ratio r. The zero-frequency window adds the unbounded coarse tail $R_B \ge 2L R_A$, or its portion below an admissible maximum radius. Every lane in

that tail participates, whether its ratio is rational or irrational. At $R_B = 300R_A$ and $L = 100$, $q_L = 1$ and the coherence is about 0.827, above the coarse-tail lower bound $2/\pi \simeq 0.637$.

At a common sweep event, the synchronized reference repeats its starting phase on the N rays $\beta_X + 2\pi j/N$. For $r = p/q$, equal-path samples return to this set every q samples; for irrational r, only the starting sample lies on it. The return can be to a different ray in the set. The baseline orientation and its retention mechanism lie beyond this phase recurrence.

A comparison over k reference circuits contains $L = kN$ samples when its final endpoint is excluded. Increasing k, or increasing N at fixed k, narrows the finite-window tolerances.

7. INTERPOLATION AND THE TRANSITION BAND

7.1 Joining samples on the record circle

[D] **Straight-line reading convention.** Join consecutive phase samples by straight segments in the complex plane of the record circle.

The convention is motivated by the straight distance rays of scale space, but it is an additional assumption: a geometric distance ray and a chord between phase records belong to different representations. If a resolved phase record were interpolated along its correct forward arcs instead, the interpolation error studied here would vanish.

For a correctly reconstructed lane, $0 < r < 1$, successive phases are separated by the forward angle $2\pi r$. At matching fractions of the sampling interval, the largest separation between this circular course and its straight interpolant occurs at the midpoint:

$$\xi(r) = 1 - \cos(\pi r)$$

The ratio of chord length to forward arc length is

$$\frac{\sin(\pi r)}{\pi r}$$

Appendix A.4 gives the geometry. The depth ξ is measured in units of record-circle radius. For $r > 1/2$, it compares the chord with a forward arc longer than a semicircle and can exceed one, so it measures more than the chord's radial dip toward the origin.

The chord's angular order agrees with the minimal-step reading. At $r = 1/2$ it passes through the origin and the sense is undecided. For $1/2 < r < 1$, it reads in reversed order.

Samples per cycle $1/r$	**Artifact depth** ξ	**Chord/arc length**	**Form**
Between 1 and 2	Between 1 and 2	Below $2/\pi$	reversed order
2	1	0.637	diameter
4	0.293	0.900	square
8	0.076	0.974	octagon
16	0.019	0.994	regular 16-gon

For integer oversampling $1/r = k \geq 2$, the record closes into the regular k-gon, with the two-vertex case understood as a diameter. At small r, $\xi \simeq \pi^2 r^2/2$.

7.2 Amplitude dips and beats

For an amplitude record with $r \leq 1/2$, the same expression describes a worst-case sampled peak deficit. A sample lies within phase πr of a peak, giving a value at least $\cos(\pi r)$ there. The least favorable alignment places two samples equally far from that peak. At Nyquist, samples on zero crossings can make the entire record zero.

Every phase-record chord has the same geometric depth. Its projection on a coordinate axis depends on the starting phase, so amplitude dips can vary from cycle to cycle. Near integer oversampling k, their slow modulation is associated with the drift of z_m^k, with characteristic scale

$$L_{\text{beat}} \sim \frac{1}{d_{\mathbb{Z}}(kr)}$$

when the denominator is small and nonzero. This is a phase-drift scale; an exact repetition period additionally requires commensurability. For $r = 10/41$, $d_{\mathbb{Z}}(4r) = 1/41$ gives a drift scale of 41 samples, which here coincides with the exact period. A small change in the sampler can greatly change this scale while barely changing ξ, as Appendix B.5 shows.

7.3 A tolerance sets the settling threshold

[D] Choose an interpolation tolerance $0 < \xi_{\text{tol}} < 2$.
The reading settles when $\xi(r) \leq \xi_{\text{tol}}$, or

$$R_B \geq R_{\text{st}} \qquad R_{\text{st}} = \frac{\pi R_A}{\arccos(1 - \xi_{\text{tol}})}$$

The interval $R_A < R_B < R_{\text{st}}$ is the phase-record transition band. This paper adopts

$$\xi_{\text{tol}} = 1 - \cos(\pi/8) \simeq 0.07612 \qquad R_{\text{st}} = 8R_A$$

At this reference tolerance the band spans three octaves. The amplitude reconstruction boundary is $2R_A$, leaving two octaves to the same threshold. A one-percent tolerance moves the threshold to about $22.2R_A$, so the three-octave width is a benchmark chosen through the tolerance, distinct from an independently predicted constant.

[I] The eightfold benchmark was selected to match the onset of stability reported in earlier exploratory simulations of the framework. A simulation using the same interpolation rule and tolerance reproduces it by construction. An independent stability test must use a separate criterion, such as estimation error under noise.

7.4 Four relational regimes

[D] With phase records, the stated branch convention, and the reference tolerance, classify an ordered pair of lanes and record length as follows:

Regime	Condition	What the classification says
Resolved	$R_B \geq 8R_A$	correct branch reconstruction; interpolation within tolerance
Transitional	$R_A < R_B < 8R_A$	correct branch reconstruction; interpolation exceeds tolerance
Locked	$R_B \leq R_A$ and $q_L 2 \leq L$	hidden alias rung; low-order recurrence
Diffuse	$R_B \leq R_A$ and $q_L 2 > L$	hidden alias rung; recurrence only beyond the low-order cutoff

The name resolved regime includes a stability condition. Correct scale reconstruction alone holds in both the resolved and transitional regimes.

Two axes organize this table: whether the selected branch returns the true scale, and whether the chosen record statistic is stable. Interpolation error supplies that statistic above the reconstruction boundary; low-order coherence supplies it below. They are different measures, each tied to its side of the reconstruction boundary.

A small ratio change shifts the phase of sample m by $2\pi m \Delta r$ in every regime. Sample-by-sample phase agreement therefore holds over windows with $m|\Delta r|$ well below one half, in every classification, and a finite-window lock can dissolve as the record extends.

With amplitude records, the reconstruction boundary moves to $2R_A$ and the transitional interval is $2R_A < R_B < 8R_A$; the recurrence cutoff can still classify the aliased side. These labels describe the relation to a sampler. One lane can occupy different regimes for different reference scales.

8.1 Scale acceleration and accumulated distance

[D] **Postulate 11: Acceleration.** A system accelerates in the model when its radius increases along its retained baseline. With continuous sweep-cycle coordinate $n = \Theta/(2\pi)$, define

$$\alpha_n = \frac{dR}{dn}$$

The stride per sweep cycle is $\sigma(R) = 2\pi R$. Accumulated lane distance is its integral,

$$S(n) = \int_0^n 2\pi R(n')\, dn' \qquad \frac{dS}{dn} = 2\pi R \qquad \frac{d^2S}{dn^2} = 2\pi\alpha_n$$

The straight displacement along the baseline is instead $\Delta = R(n) - R_0$. The two distances have different meanings. Moreover, S counts circumferential travel, while the full Euclidean spiral would have line element

$$ds_{\text{spiral}} = \sqrt{\alpha_n^2 + (2\pi R)^2}\, dn$$

Under the local-duration rule,

$$\frac{d\tau}{dn} = \frac{2\pi R}{c} \qquad S = c\tau$$

Thus lane travel remains at c in accumulated local duration. Growing scale increases the lane distance covered per sweep cycle.

8.2 Constant scale growth and the squared-scale law

For constant $\alpha > 0$,

$$R(n) = R_0 + \alpha n \qquad S(n) = 2\pi R_0 n + \pi\alpha n^2$$

Eliminating n gives

$$R^2 = R_0^2 + \frac{\alpha}{\pi} S = R_0^2 + \frac{\alpha c}{\pi} \tau$$

Equivalently,

$$S = \frac{\pi}{\alpha} \Delta (D_0 + \Delta) \qquad D_0 = 2R_0$$

A prescribed lane distance S_1 is reached after

$$n = \frac{\sqrt{R_0^2 + \alpha S_1/\pi} - R_0}{\alpha}$$

fewer sweep cycles than $S_1/(2\pi R_0)$ at fixed scale. Both histories still assign local duration S_1/c to that same accumulated lane distance.

Defining $a_\sigma = 2\pi\alpha$ gives the formal kinematic identity

$$\sigma^2 = \sigma_0^2 + 2a_\sigma S$$

Here the parameter is sweep cycles and the velocity-like quantity is stride. The identity is formal and stops short of a derivation of Newtonian acceleration: $\Delta = \alpha n$ has zero second derivative in n, while $dS/d\tau = c$ stays constant.

With the instantaneous cycle duration $T = 2\pi R/c$,

$$S = \frac{c^2(T^2 - T_0^2)}{4\pi\alpha} \qquad \frac{d(R^2)}{d\tau} = \frac{\alpha c}{\pi} \qquad \frac{dR}{d\tau} = \frac{\alpha c}{2\pi R}$$

Curvature falls as the lane grows:

$$\frac{d\kappa}{dn} = -\alpha_n \kappa^2 \qquad \frac{1}{\kappa^2} = \frac{1}{\kappa_0^2} + \frac{\alpha}{\pi} S$$

with the second relation for constant α. The deflection c^2/R falls with it, while the circumference-to-diameter ratio remains π.

8.3 An accelerating sampler

Let A grow as $R_A(n) = R_0 + \alpha n$ while B stays fixed. The sampling ratio is $(R_0 + \alpha n)/R_B$. It crosses integers at

$$n_k = \frac{kR_B - R_0}{\alpha} \qquad \Delta n_{\text{lock}} = \frac{R_B}{\alpha}$$

The reference transition interval for a fixed B is crossed while $R_B/8 < R_A(n) < R_B$. The alias boundary occurs at $n = (R_B - R_0)/\alpha$ when the initial sampler is smaller than B.

For a changing sampler, sample paths must accumulate its changing wavelengths:

$$s_m = \int_0^{m/N} 2\pi R_A(n)\, dn$$

Define $r_0 = R_0/R_B$ and $\eta = \alpha/(NR_B)$. The record phase is exactly

$$\vartheta_m = \frac{Ns_m}{R_B} = 2\pi r_0 m + \pi \eta m^2$$

up to a constant. Multiplying m by the current wavelength would double the quadratic term and give a different sampling rule.

Each sampled step reads the ratio at the midpoint of its interval:

$$\vartheta_{m+1} - \vartheta_m = 2\pi \left[r_0 + \eta \left(m + \frac{1}{2} \right) \right]$$

At an integer crossing, the record is $e^{i\pi\eta m^2}$ up to constant phase. For slow variation, $\eta \ll 1$, the accumulated drift becomes substantial at ηL^2 of order one. This gives the coherence-length estimate

$$L_{\text{lock}} \sim \eta^{-1/2} = \sqrt{\frac{NR_B}{\alpha}}$$

Its numerical coefficient depends on the coherence threshold and placement of the window. Appendix A.5 distinguishes a window beginning at a crossing from one centered on it.

In this slow regime, the minimal-step reading passes through near-stationarity, forward drift, undecided order, reversed drift, and another near-lock. Faster changes can alias the quadratic phase itself: integer r_0 and $\eta = 2$ give a stationary record for every sample. More generally, rational r_0 and η with common denominator Q give a periodic record with period dividing $2Q$. These exact sampling identities concern the record, while the radius itself keeps changing.

9.1 An optional geometric extension

[D] The preceding results use perfect circular lanes. An optional displacement amplitude $\zeta \geq 0$ offsets a lane by $\zeta \sin\Phi$. This amplitude has units of length and is distinct from the imprint amplitude A_0.

A radial offset spreads the lane across radii $R \pm \zeta$. A transverse offset along an additional internal direction would keep its scale, but that direction belongs to the unfinished geometry of a slice. Both constructions have the same leading path excess.

[D] **Postulate 8′: Duration on a displaced lane.** In the frame where the displaced pattern is stationary, assign local duration $d\tau = ds_\zeta/c$ to traversal of its arc element. Write $g_R = ds_\zeta/d\Theta$. For a transverse offset,

$$g_R(\Phi) = \sqrt{R^2 + N^2\zeta^2\cos^2\Phi}$$

For a radial offset, replace R^2 under the square root by $(R + \zeta\sin\Phi)^2$. The circuit length C_ζ and path factor F_R obey, for $N\zeta/R \ll 1$,

$$C_\zeta = 2\pi R + \frac{\pi N^2\zeta^2}{2R} + \cdots \qquad F_R = \frac{C_\zeta}{2\pi R} \simeq 1 + \frac{N^2\zeta^2}{4R^2}$$

The mean progress around the reference circle is

$$\bar{v} = \frac{c}{F_R} \qquad \sqrt{1 - \frac{\bar{v}^2}{c^2}} \simeq \frac{N\zeta}{\sqrt{2}R}$$

The path excess and the fractional reduction $1 - \bar{v}/c \simeq N^2\zeta^2/(4R^2)$ are quadratic in amplitude. The last quantity, the zig-zag share, is linear to leading order: it equals the root-mean-square slope of the displaced lane against the reference circle, the share of motion at c carried across the mean direction. The perfect lane is recovered at $\zeta = 0$.

9.2 Clock corrections

Under Postulate 8′, the phase still advances uniformly with sweep phase and, in general, nonuniformly with local duration. One circuit lasts C_ζ/c, giving

$$\bar{f}_R = \frac{Nc}{2\pi R F_R} \qquad \frac{\bar{f}_B}{\bar{f}_A} = \frac{R_A F_A}{R_B F_B}$$

The phase-order density averaged along the displaced path is N/C_ζ. Perfect-lane sampling formulas therefore hold exactly at zero displacement and approximately at small displacement.

For a transverse offset, put $\epsilon = N\zeta/R$ and let $\bar{\Phi} = 2\pi \bar{f}_R \tau$ with a suitable phase origin. Then

$$\Phi = \bar{\Phi} - \frac{\epsilon^2}{8}\sin(2\bar{\Phi}) + O(\epsilon^4)$$

The relative rate modulation has amplitude $\epsilon^2/4$ and the phase deviation has amplitude $\epsilon^2/8$ radians. A radial offset adds first-order modulation of size ζ/R, including a phase deviation of that size at the imprint frequency. Sampling displaced lanes must account for the nonuniform phase-to-path relation of both sampler and sampled lane; the circuit-averaged ratio supplies only the mean comparison.

9.3 The mass conjecture

[C] A proposed mass interpretation adds two assumptions. First, a scale mode carries energy E_R moving at c along its lane, and its time-averaged tangential circulation momentum is identified as

$$p_R = \frac{E_R \bar{v}}{c^2}$$

Second, this scalar circulation quantity is used as the momentum in the relativistic energy–momentum relation. The resulting assigned rest energy is

$$m_R c^2 = \sqrt{E_R^2 - c^2 p_R^2} = E_R \sqrt{1 - \frac{\bar{v}^2}{c^2}} \simeq \frac{E_R N \zeta}{\sqrt{2} R}$$

Under these assumptions, the perfect lane is massless and the assigned mass grows linearly with ζ at fixed E_R, N, R. A universal law $m_R = K\zeta$ would additionally require $E_R N/R$ to be constant.

Both momentum identifications are assumptions beyond the geometric calculation. Circulation projected onto a rotating tangent differs in general from the net momentum of a physical system. In a complete closed system with total momentum zero, the invariant

mass instead equals total energy divided by c^2, including the energy of whatever maintains the circulation. If that total energy were E_R, even a perfect lane would have mass E_R/c^2 under that alternative reading.

Zitterbewegung and zig-zag interpretations motivate the comparison [8–10], while the momentum that belongs to the proposed mode remains for the conjecture to establish. A test requires an independent determination of E_R and ζ, followed by a mass prediction for a system outside the calibration set. A phase-based energy such as a Planck form remains an additional hypothesis to examine.

9.4 Defined sweep energy

[D] Define

$$E_R^{\mathrm{SW}} = m_R(R\Omega)^2 = m_R\,|x^+|\,|y^+|\,\Omega^2$$

where the two coordinate magnitudes equal R. It has energy units and satisfies $E_R^{\mathrm{SW}}/(m_R c^2) = (R/R_*)^2$.

[C] Reading this quantity as physical energy in sweep time requires an energy-conversion rule. On perfect lanes $d\tau/dt = R/R_*$. An energy defined as phase rate times a fixed action constant converts with one power of this factor. A dimensional conversion holding mass and length fixed gives two powers and requires a corresponding treatment of the action constant. These are different conventions.

For a displaced lane the instantaneous factor is $g_R(\Phi)/R_*$ and its sweep-cycle average is RF_R/R_*. The defined quantity E_R^{SW} is retained here; its identification with measured energy remains open. The test is to derive the conversion from a specified clock-energy rule and compare it with the proposed squared factor.

[D] If m_R remains constant during scale growth, the squared-scale law gives

$$E^{\mathrm{SW}} = E_0^{\mathrm{SW}} + \frac{m_R\Omega^2\alpha}{\pi}S$$

Here S is mean-circle lane distance. Along the displaced path, $dS_\zeta = C_\zeta\,dn$ and

$$\frac{dE^{\mathrm{SW}}}{dS_\zeta} = \frac{m_R\Omega^2\alpha}{\pi F_R}$$

The linear relation resembles a work–energy law, while physical work requires a force or transfer mechanism that this definition leaves open.

The displaced-lane circumference divided by the reference diameter is πF_R. A radial lane's actual largest diameter is $2(R + \zeta)$ for even N; for odd N this is an upper bound. Its ratio to that diameter can differ from π. Appendix A.6 states the small-amplitude comparison, keeping it separate from the exact circular geometry of the core model.

10. PHYSICAL INTERPRETATIONS & THE RESEARCH PROGRAM

10.1 The proposed quantum–classical connection

[C] The central hypothesis associates classical behavior with records that are both correctly reconstructed and stable, and quantum ambiguity with relations whose true scale occupies a hidden alias rung. A low-order lock combines ambiguity with recurrence; a transitional record combines correct reconstruction with interpolation error above the selected tolerance.

This interpretation goes beyond aliasing alone. Classical signal processing also produces alias families, and a probability law for their members remains to be supplied. Identifying these alternatives with quantum alternatives requires a weighting rule and quantitative agreement with quantum experiments.

The proposed divide is relational: changing the sampler moves the reconstruction boundary and the interpolation threshold in proportion to R_A. At the reference tolerance, their separation is three octaves for phase records and two for amplitude records. To test a physical correspondence, one must identify the scales of an apparatus and a sampled system independently, then examine whether the observed crossover follows that scaling. The stability criterion must be independent of the tolerance used to define the band.

Several structures suggest possible comparisons: overlap between records, the inverse relation between overlap width and record length, discrete alias alternatives, and the addition of a second sampler to select an alternative. A quantum state space, a Born rule, and a measurement theory remain to be established. Likewise, stroboscopic averaging is a kinematic filter; relating it to environment-induced decoherence requires an environmental interaction model [11].

10.2 From recurrence to enduring systems

[C] The baseline picture requires a mechanism that retains an orientation after the sweep has passed, distributes the signal outward, and specifies its delay in a declared time measure. A single ray that rotates with the sweep provides one orientation at a time, while distinct systems use several retained orientations.

The participation rule also requires dynamics before it can describe enduring objects. Its membership depends on A and L, includes nearly stationary coarse lanes, and can change

when the record length changes. A physical system would need a persistence condition or a coupling law that maintains the relevant relations.

Coupled phase models can have attractive mode-locking regions, including Arnold tongues [12]. Such coupling is an additional ingredient. A simulation must distinguish the recurrence windows $|r - p/q| \leq 1/(2qL)$ from windows produced by a coupling strength. The latter require evidence beyond the former.

10.3 Acceleration, curvature, and spacetime

[C] A geometrical parallel connects lane deflection with uniform proper acceleration. In Minkowski spacetime, a uniformly accelerated trajectory has $x^2 - c^2t^2 = c^4/a^2$ [13]. Continuation to imaginary time gives a circle of radius c^2/a and period $2\pi c/a$ in Euclidean proper time. A lane with $a_R = c^2/R$ has exactly that radius and local period. Appendix A.7 shows the correspondence.

In quantum field theory, the associated Unruh temperature is $k_B T = \hbar a/(2\pi c)$ [14, 15]. Matching the circular period leaves the thermal response to be derived. A meaningful next test is a derivation of a detector response or spectrum from the model's own stated assumptions.

Lane curvature also differs from intrinsic spacetime curvature: uniformly accelerated observers can occupy flat spacetime. A route toward gravitational field equations would require a rule that combines lane relations into a metric of distance rays and produces intrinsic curvature. The current model leaves this rule open.

Similarly, cycle-based scale acceleration must be connected to measured acceleration through an explicit clock and length calibration. The greater local duration accumulated at larger radius over the same sweep interval is a property of the present duration rule; its relation to relativistic proper time between fixed physical events remains to be established.

10.4 Shared modes and entanglement

[C] One possible extension reads entangled particles as positions of one shared scale mode. Membership requires more than equal radius: every pair of positions on a lane already shares the synchronized phase relation $-N\Delta\beta$.

The extension needs a joint-mode definition, a rule for local readout, and a rule for how a measurement changes the mode. A preassigned common phase with local readouts and

measurement settings independent of that phase obeys the CHSH bound 2. Quantum theory allows a maximum $2\sqrt{2}$ [16–18]. The required quantum correlations therefore need more than the shared phase relation.

Suppose, additionally, that a disturbance travels around the lane at angular rate Ω. For directed angular separation $0 < \theta < 2\pi$,

$$\Delta t = \frac{\theta}{\Omega} \qquad \Delta\tau_R = \frac{R\theta}{c}$$

The path speeds $R\Omega = (R/R_*)c$ and c express one motion using different clocks. Measured with lane duration and the straight endpoint distance,

$$\frac{d}{\Delta\tau_R} = c\,\frac{2\sin(\theta/2)}{\theta} \le c$$

A claim of faster-than-light influence therefore needs an operational mapping to laboratory clocks and distances. Baseline information transport at c needs its time measure specified as well. The two channels must be compared under the same measurement procedure. Giving a disturbance the sweep's angular rate is a new transport assumption, beyond the rotation of an undisturbed phase pattern.

Experiments cited in [19, 20] constrain hypothetical finite-speed influences to roughly $10^4 c$ or more for the stated class of preferred frames in which Earth's speed is below $10^{-3}c$. These bounds concern influences of fixed speed in a preferred inertial frame under those conditions, a narrower class than all conceivable finite-speed influences; a scale-dependent speed such as $(R/R_*)c$ needs its own analysis. Whether entanglement uses a travelling influence at all remains open. Applying those bounds to STT requires a mapping from lane events to detector separations and timestamps.

A further constraint comes from four-party correlations. Under the finite-speed causal structure studied in [21], reproducing quantum predictions when the events can exchange influences conflicts with no-signalling. The argument already allows correlations to fail where the proposed influence arrives too late. A no-signalling extension must identify which further prediction or causal assumption it changes, and show that the lane dynamics realizes, or differs from, the structure addressed by that theorem.

The immediate development task is therefore the joint-mode and readout rule. An entanglement mechanism and a physical propagation speed remain open.

10.5 What remains to be specified

The open foundations can be grouped into five tasks.

Task	Required development
Complete the geometry	Define the second internal direction of a finite, borderless slice, its normal, and any admissible minimum or maximum scale, and state how distance rays combine into a spacetime metric of Lorentzian signature.
Specify physical access	Identify the carrier of the imprint, access to wrapped phase, and how equal-path sampling and interpolation are implemented.
Supply dynamics	Explain baseline retention, outward delivery, coupling, system persistence, and changing-path delays, for instance through an action principle on the chart $(0,\infty) \times S1$.
Calibrate observables	Relate R_*, Ω, N, χ and the two time measures to measured length, time, acceleration, and light propagation.
Define quantum and energetic rules	Assign weights to alternatives and state the conditions under which they reproduce the Born rule, specify joint-mode measurement, identify physical momentum, and determine E_R independently of mass.

The phasor's ontology remains part of these tasks: it may be a physical field, a boundary condition, a geometric reference, or a device for expressing shared order. Deciding among them requires more than the current equations.

10.6 A validation sequence

The sampling construction can be checked before proposing physical correspondences. A simulation should first build the imprint on lanes and sample it along equal paths, then compare those results with clock readings at equal local durations. It should recover the alias families, recurrence windows, interpolation depths, and accumulated-path acceleration formulas.

A second stage should add explicit readout noise and estimate scale or residual from finite records. Noise added to wrapped phase and noise added independently to the two complex coordinates define different experiments. Phase noise on the circle, for instance von Mises distributed, keeps every sample on the unit circle; complex Gaussian noise added to z_m moves samples off it and calls for a phase-extraction step, $\arg z_m$, or an estimator that also uses the magnitude. Stability should be measured by estimation error or another criterion chosen independently of the reference interpolation tolerance.

A third stage can test proposed extensions separately: coupled dynamics, displaced-lane clocks, joint modes, or candidate probability weights. A noise-smoothed outcome curve resembling a quantum probability law falls short of a derivation of that law, which must follow from stated assumptions across noise levels, record lengths, and sampling depths.

Physical tests then require independent calibration and predictions for systems outside the calibration set. The analytical checks and worked examples of this paper establish internal relations only.

11. CONCLUSION

STT 12.0 provides a kinematic model in which one shared phase order is distributed over lanes of different size. Equal-path comparison turns their phase-order densities into the sampling ratio R_A/R_B. Wrapped phase records then yield alias families, apparent reversal, rational recurrence, and finite-window coherence. A chosen interpolation rule adds a tolerance-dependent transition band. Scale growth gives a squared-scale law, while optional lane displacement supplies a separate geometric basis for exploring mass.

These results distinguish assumptions about access and reading from their mathematical consequences. They also locate the proposed physical connections: a quantum–classical interpretation needs calibrated observables and probability rules; enduring systems need dynamics; mass needs a justified momentum assignment; and entanglement needs a joint-state and readout mechanism. The framework's next step is to make those additions explicit and test them against evidence beyond the sampling construction.

APPENDIX A. DERIVATIONS

A.1 Equal paths and local clock readings

At sweep phase Θ_0, the point a distance s behind the baseline of B has angle $\beta_B - s/R_B$. Its imprint phase is

$$N\left(\Theta_0 - \beta_B + \frac{s}{R_B}\right) + \phi_0$$

Putting $s = m\lambda_A = 2\pi m R_A/N$ gives the increment $2\pi m R_A/R_B$. At the baseline, elapsed local duration s/c advances sweep phase by s/R_B and gives the same imprint phase. This establishes the spatial and equal-local-duration forms of the record. A fixed received-phase offset adds only to the constant term.

A.2 The window and its bounds

For noninteger x, summing the geometric progression gives

$$\sum_{m=0}^{L-1} e^{2\pi i x m} = e^{\pi i x(L-1)} \frac{\sin(\pi L x)}{\sin(\pi x)}$$

Taking its magnitude and dividing by L yields Γ_L. Integer shifts and sign reversal of x leave it unchanged, so put $y = d_{\mathbb{Z}}(x) \in (0,1/2]$.

Jordan's inequality gives $\sin(\pi y) \geq 2y$. Bounding the numerator by one yields $\Gamma_L \leq 1/(2Ly)$. If $y \leq 1/(2L)$, apply the same inequality to the numerator and use $\sin(\pi y) \leq \pi y$:

$$\Gamma_L(x) \geq \frac{2Ly}{\pi Ly} = \frac{2}{\pi}$$

At $y = 0$ the value is one. Substituting $x = r - r'$ gives the overlap bounds, since the constant phase difference factors out before taking the magnitude. Substituting $x = qr$ gives order-q coherence.

The bound $q_L \leq 2L - 1$ also follows geometrically. Place the $2L$ fractional parts $0, r, \ldots, (2L-1)r$ on a circle of circumference one. Two neighboring points have circular separation at most $1/(2L)$; their index difference is an eligible q between 1 and $2L - 1$.

A.3 Two samplers

The first sampler fixes r modulo one, so alternative ratios differ by an integer j. The second fixes μr modulo one, with $\mu = R_{A'}/R_A$. An alternative survives both exactly when μj is an integer.

For irrational μ, only $j = 0$ survives. For reduced $\mu = p'/p$, survival requires p to divide j, so the pair determines r modulo p. This proof assumes exact ratios and noiseless records; a uniform finite-noise separation between all candidates requires a further argument.

A.4 Interpolation geometry

Rotate the initial sample to one and write the next as $e^{2\pi i r}$. At interval fraction $u \in [0,1]$, compare the forward circle $e^{2\pi i r u}$ with the interpolant $(1-u) + u e^{2\pi i r}$. At $u = 1/2$,

$$\frac{1 + e^{2\pi i r}}{2} = \cos(\pi r) e^{\pi i r}$$

Its separation from the arc midpoint $e^{\pi i r}$ is $1 - \cos(\pi r)$. To evaluate the full interval, put $a = \pi r$ and $v = 2u - 1$. After rotation by $-a$, the squared separation is

$$E^2(v) = [\cos(av) - \cos a]^2 + [\sin(av) - v \sin a]^2$$

For $0 < a < \pi$, its maximum on $[-1,1]$ occurs at $v = 0$, giving the stated depth. The chord length is $2\sin(\pi r)$ and the forward arc length is $2\pi r$. Their ratio also equals the magnitude of the average phase over the interval:

$$\frac{1}{2\pi r} \int_0^{2\pi r} e^{i\theta}\, d\theta = e^{\pi i r} \frac{\sin(\pi r)}{\pi r}$$

For small r, $\xi = \pi^2 r^2/2 - \pi^4 r^4/24 + \cdots$. Solving $\xi \le \xi_{\text{tol}}$ gives Section 7.3; for small tolerances, $R_{\text{st}} \simeq \pi R_A / \sqrt{2\xi_{\text{tol}}}$.

A.5 Growth and quadratic records

For constant scale growth, $dS/dR = (dS/dn)/(dR/dn) = 2\pi R/\alpha$. Integrating gives $S = (\pi/\alpha)(R^2 - R_0^2)$. A stepwise sum using midpoint radii $R_i = R_0 + \alpha(i + 1/2)$ reproduces the continuous result at integer cycle counts. Starting-point radii instead give $2\pi R_0 n + \pi\alpha n(n-1)$, short by $\pi\alpha n$.

At sample m, $n = m/N$, and

$$\tau_A = \frac{2\pi}{Nc}\left(R_0 m + \frac{\alpha m^2}{2N}\right) \qquad s_m = c\,\tau_A$$

Multiplying by the fixed lane's angular clock rate $2\pi f_B$ gives $2\pi r_0 m + \pi\eta m^2$. Summing ratios held at the beginning of each interval would give $2\pi r_0 m + \pi\eta m(m-1)$, differing by the linear term $\pi\eta m$.

For a long window beginning at an integer crossing, let $a = \eta L^2$ be fixed. Its coherence approaches

$$\left|\int_0^1 e^{i\pi a x^2}\,dx\right|$$

At $a = 1$ this is about 0.628, close to but below $2/\pi$. A window centered on the crossing instead approaches

$$\left|\int_{-1/2}^{1/2} e^{i\pi a x^2}\,dx\right|,$$

about 0.973 at $a = 1$. Thus the inverse-square-root length is a scaling estimate, distinct from the exact finite-window bound of Section 6.

For rational $r_0 = a_0/Q$ and $\eta = b_0/Q$, shifting m by $2Q$ changes the phase by an integer multiple of 2π, proving the stated period bound. Special cases may have shorter periods.

A.6 Displaced paths and clocks

At fixed sweep phase, let $\Phi = N\beta + \phi$; the circuit length is independent of the sign and constant. The two path elements are

$$ds_\perp = \sqrt{R^2 + N^2\zeta^2\cos^2\Phi}\,d\beta$$

$$ds_{\text{rad}} = \sqrt{(R + \zeta\sin\Phi)^2 + N^2\zeta^2\cos^2\Phi}\,d\beta$$

For fixed positive integer N and $\zeta/R \ll 1$, expansion and integration give, in both cases,

$$C_\zeta = 2\pi R + \frac{\pi N^2 \zeta^2}{2R} + O(\zeta^4/R^3)$$

where the dimensionless coefficient in the remainder depends on N. In the radial case the second-order $\sin^2\Phi$ terms cancel, so the ζ^2 coefficient equals the transverse one and the two lengths differ at fourth order. The expansion used in the main text requires $N\zeta/R \ll 1$ as well. Odd powers of ζ integrate to zero, since a half-period shift of the phase origin reverses the sign of ζ.

For a transverse offset, $d\Phi/d\tau = Nc/g_R$ and $\epsilon = N\zeta/R$. Expanding gives

$$\frac{d\Phi}{d\tau} = \frac{Nc}{R}\left[1 - \frac{\epsilon^2}{4} - \frac{\epsilon^2}{4}\cos(2\Phi) + O(\epsilon^4)\right]$$

Integration with a suitable origin gives $\bar{\Phi} = \Phi + (\epsilon^2/8)\sin(2\Phi) + O(\epsilon^4)$, and inversion gives the phase correction in Section 9.2.

Radial displacement gives at first order $\Phi = \bar{\Phi} + (\zeta/R)\cos\bar{\Phi}$, up to a constant phase choice.

For the circulation-momentum construction, the time average of the tangent component of a unit velocity is $2\pi R/C_\zeta$. For a transverse offset this follows directly by integrating the reference-circle increment. For the radial offset the tangential increment integrates as

$$\int_0^{2\pi} (R + \zeta\sin\Phi)d\beta = 2\pi R.$$

Multiplication by the assumed local momentum E_R/c gives the scalar p_R of Section 9.3. Interpreting it as the system's physical momentum remains the separate conjecture stated there.

For an even-N radial displacement, the largest diameter is $2(R + \zeta)$. Its length ratio is

$$\frac{C_\zeta}{2(R+\zeta)} \simeq \pi\,\frac{1 + N^2\zeta^2/(4R^2)}{1 + \zeta/R}$$

Within the small-amplitude expansion, this is below π when $\zeta < 4R/N^2$ and above it when the opposite inequality holds within the same validity range. For odd N, the denominator is only an upper bound on the diameter, so the same expression is a lower bound on the actual length-to-diameter ratio.

A.7 The imaginary-time circle

For uniform proper acceleration a, the standard trajectory is [13]

$$x(\tau) = \frac{c^2}{a}\cosh\frac{a\tau}{c} \qquad ct(\tau) = \frac{c^2}{a}\sinh\frac{a\tau}{c}$$

Under $t = -it_E$ and $\tau = -i\tau_E$ it becomes

$$x = \frac{c^2}{a}\cos\frac{a\tau_E}{c} \qquad ct_E = \frac{c^2}{a}\sin\frac{a\tau_E}{c}$$

Its radius, angular rate, and period match $R = c^2/a_R$, $c/R = a_R/c$, and $2\pi c/a_R$ for a scale-lane. This geometrical identity is the extent of the derived comparison. The field-theoretic thermal interpretation requires additional structure [14, 15].

APPENDIX B. WORKED EXAMPLES

B.1 One sampler and ten lanes

Set $R_A = 1$ and use the reference interpolation tolerance. The irrational radii and the radius corresponding to $r = 3.01$ are specified exactly below, so their locking orders hold independent of rounding.

R_B	r	w	ρ	δ	R^{app}	q_{50}	q_{100}	Regime at $L = 100$
10	0.1	0	0.1	0.1	10	10	10	resolved
4	0.25	0	0.25	0.25	4	4	4	transitional
3/2	2/3	0	2/3	$-1/3$	3/2	3	3	transitional
1	1	1	0	0	∞	1	1	locked, self
1/2	2	2	0	0	∞	1	1	locked
2/5	5/2	2	1/2	-1/2	2	2	2	locked
3/10	10/3	3	1/3	1/3	3	3	3	locked
100/301	3.01	3	0.01	0.01	100	1	100	diffuse
$2/(1+\sqrt{5})$	$(1+\sqrt{5})/2$	1	0.618…	$-0.382\ldots$	1.618…	55	144	diffuse
$1/\sqrt{2}$	$\sqrt{2}$	1	0.414…	0.414…	2.414…	70	169	diffuse

The first three rows have artifact depths about 0.049, 0.293, and 1.5. The third is correctly reconstructed by the forward branch while its minimal-step reading reverses. The ratio 3.01 is an order-one lock at $L = 50$ and reaches order 100 at $L = 100$, illustrating the role of the observation window.

B.2 An alias ladder and another sampler

For $R_B = 0.3$ and $R_A = 1$, the residual is $1/3$. The alias family begins

$$3, \quad 0.75, \quad 0.428571\ldots, \quad 0.3, \quad 0.230769\ldots, \quad 0.1875$$

The true radius occupies rung $j = 3$, while the forward reading returns 3. A second sampler at $R_{A'} = \sqrt{2}$ has residual about 0.714045;
its family begins 1.9806,0.8251,0.5211,0.3808,0.3,0.2475,…. With $R_{\min} = 0.01$, the families contain 100 and 141 members and intersect exactly at 0.3.

Exact uniqueness can coexist with difficult discrimination under noise. Distinct members of the two families can lie very close: a pair near 0.01364 differs by about 4.9×10^{-5} in relative radius. Their ratio separations modulo one are about 0.0036 and 0.0051 for the two samplers. The overlap bound requires respectively about 281 or 198 samples to guarantee overlap at most $1/2$ for that pair.

A commensurate second sampler at $R_{A'} = 0.5$ instead leaves ratios modulo two, including the radii 0.75,0.3,0.1875,0.1364,….

B.3 Lock tolerance and participation

At $L = 100$, an exact integer lock at $R_B = R_A/2$ tolerates $|\Delta R_A/R_A| \le 0.0025$. At $R_B = R_A/100$, the tolerance is 5×10^{-5}, fifty times tighter.

For $R_B = 20R_A$, the order is 20 at both $L = 100$ and 400. The criterion $q_L^2 \le L$ therefore excludes the slice at the shorter window and includes it at the longer. For $R_B = 300R_A$ and $L = 100$, it instead finds an order-one lock with coherence $0.827008\ldots$, above the coarse-tail bound $2/\pi$: this lane participates because its phase advances by only a third of a cycle over the window.

B.4 Scale growth

Take $R_0 = 1$, $\alpha = 0.1$ per sweep cycle, $S_1 = 100$, and $c = 1$. The fixed-scale cycle count is about 15.92. The growing lane reaches the same accumulated distance after about 10.45 cycles, at $R \simeq 2.045$.

Its local duration is 100. A companion held at $R_0 = 1$ accumulates about 65.68 over those same sweep cycles. The squared scale is $R^2 \simeq 4.183$, its straight displacement is about 1.045, and its curvature has fallen to about 0.489.

For sampled lane $R_B = 0.5$ and $N = 12$, the sampler begins at $r_0 = 2$, has $\eta = 1/60$, and crosses successive integer ratios every five sweep cycles or 60 samples. The approximate coherence length is $\sqrt{60} \simeq 7.7$ samples. Its first step after the initial crossing is already $\pi/60 \simeq 0.0524$ radians modulo 2π.

For constant assigned mass, the defined sweep energy grows from $m_R\Omega^2$ to about $4.183 m_R\Omega^2$ over the mean-circle distance $S = 100$.

B.5 Interpolation and a slow beat

With $R_A = 1$, the reference settling threshold is 8, while a one-percent tolerance gives about 22.2. At $R_B = 4.1$, $r = 10/41$ and $\xi \simeq 0.279$. Since $d_{\mathbb{Z}}(4r) = 1/41$, the record returns exactly after 41 samples, spanning ten cycles of the sampled lane.

Increasing R_A by one percent gives $r = 101/410$. The order-four drift scale becomes $1/d_{\mathbb{Z}}(4r) = 205/3 \simeq 68.3$ samples, while the artifact depth changes only to about 0.285. This longer beat scale is approximate; the full record's exact period is 410 samples. Thus a small scale change strongly shifts the rhythm of the projected artifacts while leaving the depth nearly unchanged.

At $R_B = 10.3$, the artifact depth is about 0.046, within the reference tolerance. Its order-ten drift scale is about 34 samples, but its amplitude dips remain small.

B.6 Displaced lanes

For $R = 1$ and $N = 10$, direct integration of the transverse path element gives:

Displacement ζ	Lane length C_ζ	Path factor F_R	Mean progress $\bar{v}/c$	Zig-zag share
0	6.28319	1	1	0
0.005	6.28711	1.000625	0.999376	0.0353
0.01	6.29886	1.002495	0.997511	0.0705

The leading zig-zag estimates are 0.0354 and 0.0707. The transverse phase deviations have amplitudes about 0.000313 and 0.00125 radians; the corresponding leading radial deviations are 0.005 and 0.01 radians. Radial and transverse circuit lengths differ by less than 4×10^{-7} in these examples.

For the radial lane with $\zeta = 0.01$, $C_\zeta/(2R) \simeq 3.14943$, while division by its actual largest diameter 2.02 gives about 3.11825. The reference-circle ratio and the displaced shape's ratio are different quantities. With $N = 1000$ and $\zeta = 10^{-5}$, the latter ratio is about 3.14164, above π while the small-amplitude condition still holds.

B.7 An octave ladder

Consider the exactly commensurate octave ladder $R_k = 2^k R_0$, with $u_k = u_0 + k \ln 2$. Each rung lies one octave above the previous one, and the perfect-lane sampling relations repeat from rung to rung because they depend on radius ratios alone. The ladder is a chosen ex-

ample within the continuous range of radii that the model admits, and its rungs serve as a reference grid of scales.

Seen from one rung, the rungs j octaves higher have $r = 2^{-j}$:

Rung above the reference	Ratio r	Phase record	Interpolation depth ξ
One octave	1/2	two antipodal points; sense undecided	1
Two octaves	1/4	four points forming a square	0.293
Three octaves	1/8	eight points forming an octagon	0.076
Four octaves	1/16	regular 16-gon	0.019

The three-octave rung meets the reference tolerance of Section 7.3; its reading as a physical classical boundary remains the hypothesis of Section 10.1. At a one-percent tolerance the continuous threshold lies 4.472 octaves up, so the first rung of the ladder within that tolerance lies five octaves up.

Widely separated rungs produce two forms of apparent rest. Looking j rungs down gives $r = 2^{j}$ and the exactly stationary record $z_m = e^{i\varphi}$, an exact harmonic alias. Looking j rungs up gives the phase advance $2\pi(L-1)2^{-j}$ across L samples, which appears as rest when it falls below a chosen observational tolerance, while two exact samples still distinguish it from rest. The exact locks require increasingly precise ratios: by Section 6.3, an integer lock j rungs down tolerates relative changes of the reference scale up to $|\varepsilon| \le 1/(2L\,2^{j})$. Upward recurrence takes 2^{j} samples and can exceed the available record.

Under constant scale growth, $\alpha = dR/dn > 0$, crossing one octave from R to $2R$ takes

$$\Delta S = \frac{3\pi R^2}{\alpha} \qquad \Delta\tau = \frac{3\pi R^2}{\alpha c} \qquad \Delta n = \frac{R}{\alpha}$$

so successive octaves require four times the lane distance and local duration and twice the sweep cycles, while the instantaneous cycle duration doubles. For K octaves from R_0,

$$S_{\text{total}} = \frac{\pi R_0^2}{\alpha}\left(4^{K} - 1\right)$$

In the squared scale, $\ln(R^2/R_*^2) = 2u$, so each octave of R is a factor four in R^2, and the defined sweep energy grows by 4^K when the assigned mass and Ω stay fixed. Equal sweep-cy-

cle counts per octave would require exponential growth, $dR/dn \propto R$. Two rungs exactly K octaves apart stand in the clock factor 2^{-K}, with the equal-path cycle-count ratio 2^{K}, while over equal sweep increments every lane shares the same imprint advance. Assigning physical objects to rungs requires the calibration listed in Section 10.5.

APPENDIX C. NOTATION AND ASSUMPTIONS

C.1 Assumption index

Assumption	Content	Location
Postulate 1	circular lanes in Euclidean reference geometry	2.1
Postulate 2	retained outward baselines and reference-based systems	2.2
Postulate 3	oriented coordinate frame with four principal rays	2.2
Postulate 4	lane circulation and straight distance rays	2.3
Postulate 5	one shared phasor sweep	2.4
Postulate 6	calibration $c = R_*\Omega$	2.4
Postulate 7	common closed imprint with integer winding	2.5
Postulate 8	local duration from lane path divided by c	3.1
Postulate 9	equal-path comparison from a common sweep event	3.2
Postulate 10	wavelength-spaced sampling retaining wrapped phase	4.1
Postulate 11	scale growth as cycle-based acceleration	8.1
Optional Postulate 8′	local duration along a displaced lane	9.1
Forward-branch convention	apparent radius and the zero-frequency reading	5.2
Minimal-step reading	shortest signed phase step	5.3
Straight-line reading convention	chord interpolation on the record circle	7.1
Low-order classification	$q_L 2 \le L$	6.2, 6.5
Reference interpolation tolerance	$1 - \cos(\pi/8)$	7.3

The minimal-step reading describes apparent order and is distinct from the forward branch used for scale reconstruction. The two classification choices determine membership and regime labels and serve as classifications alongside the physical postulates. The momentum and energy identifications of Section 9 are optional conjectural assumptions, and the shared-mode proposal of Section 10.4 leaves its transport law to be established.

C.2 Principal notation

Symbol	Meaning	Units or type
R, R_A, R_B, R_*	lane radii and calibration radius	length
$\beta, \beta_X, \Delta\beta$	orientation, retained baseline, relative orientation	radians
$\mathcal{S}X, \mathcal{R}X$	system and its participating radii	reference- and window-dependent sets
C, D, d, s, S, Δ	circumference, diameter, distance ray, path, accumulated lane distance, straight displacement	length
κ_R, a_R	lane curvature and deflection	inverse length; length/time^2
Θ, Ω, t	sweep phase, rate, parameter	radians; inverse time; time
τ_R, c, T_R	local duration, calibrated speed, local circuit period	time; length/time; time
N, Φ, ϕ_0, A_0	winding index, imprint phase, constant phase, imprint amplitude	integer; radians; radians; carrier-dependent amplitude
λ_R, ν_R, f_R	wavelength, phase-order density, local clock frequency	length; cycles/length; cycles/time
u	logarithmic scale $\ln(R/R_*)$	dimensionless
r, w, ρ, δ	sampling ratio, hidden winding, residual, minimal step in cycles	dimensionless
z_m, x_m, φ	phase sample, amplitude sample, constant record phase	complex unit value; real value; radians
L, q, q_L	record length, recurrence order, minimum order at length L	positive integers
Γ_L, O_L	window magnitude and record overlap	dimensionless
$\xi, \xi\mathrm{tol}, R\mathrm{st}$	interpolation depth, tolerance, settling radius	dimensionless; dimensionless; length
$n, \alpha_n, \sigma, a_\sigma$	continuous cycle count, scale growth, stride, stride increment	cycles; length/cycle; length/cycle; length/cycle^2
r_0, η	initial ratio and ratio growth per sample	dimensionless

ζ, C_ζ, F_R, g_R	displacement, displaced circumference, path factor, arc length per sweep angle	length; length; dimensionless; length
$\bar{f}_R, \bar{\Phi}, \bar{v}$	circuit-averaged frequency, uniform comparison phase, mean-circle progress	inverse time; radians; length/time
$E_R, p_R, m_R, E_R^{\mathrm{sw}}$	assumed mode energy, circulation momentum, assigned mass, defined sweep energy	energy; momentum; mass; energy

Angles and cycle counts are dimensionless in dimensional analysis. “Per cycle” and “per sample” retain the parameter meaning. The coordinate u appears in Section 3.2 and Appendix B.7; the interval fraction used in Appendix A.4 is a separate dummy variable. Likewise, the abbreviation $\epsilon = N\zeta/R$ in Section 9 is distinct from the sampler perturbation $\varepsilon = \Delta R_A/R_A$ in Section 6.

APPENDIX D. INTERPRETIVE NOTES

[I] Two origin statements motivate parts of the framework and stand apart from the postulates.

“The position of a scale-slice is defined by its acceleration and its size in c².” The primary reading treats squared size as R^2. Under constant scale growth, $S = (\pi/\alpha)(R^2 - R_0^2)$ connects it to accumulated lane distance. The equivalent expression through $c^2 T_R^2$ appears in Section 8.2. The separate identity $R = c^2/a_R$ fixes radius through lane deflection. A geometric position still requires its baseline orientation. Under the defined sweep energy and constant assigned mass, the same distance law becomes $S = \pi(E^{\mathrm{sw}} - E_0^{\mathrm{sw}})/(m_R \Omega^2 \alpha)$.

“If you find the past in the large scales, you will find the future in the small scales.” The sampling account suggests an interpretive reading: larger lanes can yield correctly reconstructed, settled records, while smaller lanes can leave hidden alias alternatives. Associating settled records with the past and open alternatives with the future remains an interpretation, distinct from a derived temporal law.

A related picture reads apparent rest as a lock and apparent motion as the drift of a lock offset. The forward, backward, and undecided orders of Section 5.3 provide the sampling vocabulary for that picture; connecting it to ordinary motion remains part of the calibration program.

REFERENCES

[1] A. Dupke, Scale-Time Theory 11.0: The Pre-Geometry of Scale Space, Scale-Time Dynamics Research, July 2026. DOI: 10.5281/zenodo.21221364.

[2] A. Dupke, Engineering Note EN-001 (kinematic aliasing), Scale-Time Dynamics Research. DOI: 10.5281/zenodo.18904052.

[3] H. Nyquist, "Certain topics in telegraph transmission theory," Transactions of the American Institute of Electrical Engineers 47 (1928) 617–644.

[4] C. E. Shannon, "Communication in the presence of noise," Proceedings of the IRE 37 (1949) 10–21.

[5] H. Weyl, "Über die Gleichverteilung von Zahlen mod. Eins," Mathematische Annalen 77 (1916) 313–352.

[6] G. H. Hardy and E. M. Wright, An Introduction to the Theory of Numbers, 6th ed., revised by D. R. Heath-Brown and J. H. Silverman, Oxford University Press, 2008.

[7] A. Ya. Khinchin, Continued Fractions, University of Chicago Press, 1964.

[8] E. Schrödinger, "Über die kräftefreie Bewegung in der relativistischen Quantenmechanik," Sitzungsberichte der Preussischen Akademie der Wissenschaften, Physikalisch-mathematische Klasse (1930) 418–428.

[9] R. Penrose, The Road to Reality: A Complete Guide to the Laws of the Universe, Alfred A. Knopf, New York, 2005, pp. 630–632.

[10] D. Hestenes, "The zitterbewegung interpretation of quantum mechanics," Foundations of Physics 20 (1990) 1213–1232.

[11] W. H. Zurek, "Decoherence, einselection, and the quantum origins of the classical," Reviews of Modern Physics 75 (2003) 715–775.

[12] V. I. Arnold, "Small denominators. I. Mappings of the circumference onto itself," American Mathematical Society Translations, Series 2, 46 (1965) 213–284.

[13] W. Rindler, "Kruskal space and the uniformly accelerated frame," American Journal of Physics 34 (1966) 1174–1178.

[14] W. G. Unruh, "Notes on black-hole evaporation," Physical Review D 14 (1976) 870–892.

[15] L. C. B. Crispino, A. Higuchi, and G. E. A. Matsas, "The Unruh effect and its applications," Reviews of Modern Physics 80 (2008) 787–838.

[16] J. S. Bell, "On the Einstein Podolsky Rosen paradox," Physics 1 (1964) 195–200.

[17] J. F. Clauser, M. A. Horne, A. Shimony, and R. A. Holt, "Proposed experiment to test local hidden-variable theories," Physical Review Letters 23 (1969) 880–884.

[18] B. S. Cirel'son, "Quantum generalizations of Bell's inequality," Letters in Mathematical Physics 4 (1980) 93–100.

[19] D. Salart, A. Baas, C. Branciard, N. Gisin, and H. Zbinden, "Testing the speed of 'spooky action at a distance'," Nature 454 (2008) 861–864.

[20] J. Yin et al., "Lower bound on the speed of nonlocal correlations without locality and measurement choice loopholes," Physical Review Letters 110 (2013) 260407.

[21] J.-D. Bancal, S. Pironio, A. Acín, Y.-C. Liang, V. Scarani, and N. Gisin, "Quantum nonlocality based on finite-speed causal influences leads to superluminal signalling," Nature Physics 8 (2012) 867–870.